

SIGNATURES OF THE BARYON ACOUSTIC OSCILLATIONS ON 21CM EMISSION BACKGROUND

XIAO-CHUN MAO^{1,2} AND XIANG-PING WU¹

Draft version February 2, 2008

ABSTRACT

The baryon acoustic oscillations (BAO) prior to recombination should be imprinted onto the 21cm emission background from the epoch of reionization through the underlying density perturbations. Using an analytical approach for both matter power spectrum (CDM+baryons) and reionization process, we demonstrate the BAO induced signatures on the power spectrum of 21cm emission fluctuations. Future low-frequency radio telescopes such as LOFAR and MWA should be able to detect these weak BAO wiggles with an integration time of ~ 1 year. A combination of the BAO measurements at different redshifts $z \approx 1000$ (CMB), $z \approx 10$ (epoch of reionization) and $z \approx 0$ (clustering of galaxies) may allow one to set more robust constraints on the determinations of cosmological parameters including dark energy and its equation of state.

Subject headings: cosmology: theory — large-scale structure of universe — diffuse radiation — intergalactic medium

1. INTRODUCTION

Prior to recombination, free electrons coupled the baryons and photons tightly through Compton scattering, and these three species moved together as a single fluid. In this relativistic plasma, the primordial small-scale perturbations propagated as sound waves, resulting in the pressure-induced oscillations. The neutral gas can still retain some memory of such acoustic oscillations even after recombination, manifesting themselves in the last scattering surface seen as the harmonic series of maxima and minima on the cosmic microwave background (CMB) at redshift $z \approx 1000$. The longest wavelength of BAO with $\lambda \approx 100$ Mpc imprinted on the large-scale structures is still visible in the local universe through the survey of 3D galaxy distributions (Eisenstein et al. 2005; Cole et al. 2005).

Because BAO can be served as an ideal cosmic ruler for many cosmological applications especially for the probe of dark energy (Hu & White 1996; Barkana & Loeb 2005; Wyithe, Loeb & Geil 2007), it is of great interest to explore how BAO evolve with cosmic time, and in particular how and when the peaks of BAO at smaller scales are washed out by emergence of larger structures. Indeed, in addition to the detections of BAO signatures in CMB at $z \approx 1000$ and galaxy spatial distributions at lower redshifts, one may be able to extract valuable information on BAO at redshifts around $z \approx 10$ from the study of 21 cm absorption/emission generated in the dark ages and epoch of reionization. This will complement our knowledge of structure formation at this important phase when galactic dark halos started to develop. The existing modes and positions of BAO at the epoch of reionization would make a sensitive diagnosis of nonlinear structures evolved by that time. Most importantly, the statistical uncertainties in the determination of cosmological parameters including dark energy and its equation of state can be significantly reduced when more

independent measurements of BAO through the epoch of reionization are incorporated with the BAO features already detected in CMB and large-scale structures of the local universe. Note that the 21 cm absorption/emission observations provide a tomographic imaging of the universe at the epoch of reionization and dark ages, yielding many independent constraints on the theory of cosmology.

The goal of this letter is to demonstrate the signatures of BAO on the redshifted 21 cm fluctuations and discuss the feasibility of detections with existing and planned low frequency telescopes such as 21CMA, LOFAR and MWA. We focus on the 21cm emission of neutral hydrogen during the process of reionization instead of the 21 cm absorption at $z > 20$ (Barkana & Loeb 2005). For the latter, the detection of BAO signatures turns to be much more difficult because of their longer wavelength and limitation of angular resolutions with existing and even future radio telescopes. A sophisticated treatment of the problem requires the detailed knowledge of the history of reionization and radiative transfer of ionizing photons through gas density field, which may be achievable by numerical simulations (e.g. Furlanetto, Sokasian & Hernquist 2004). Here we would rather employ an analytic approach to simplify the problem and highlight the essentials of physical process at the epoch of reionization. Throughout the paper we adopt a concordance cosmology of $\Omega_0 = 0.265$, $\Omega_\Lambda = 0.735$, $\Omega_b = 0.044$, $h = 0.71$, $n_s = 1$ and $\sigma_8 = 0.772$, as revealed by the WMAP three-year observations (Spergel et al. 2007).

2. MATTER POWER SPECTRA

We begin with the linear matter power spectrum $P_{\text{lin}}(z, k) \propto D^2(z)k^{n_s}T^2(k)$, which describes how the initial matter power spectrum k^{n_s} is modulated by the transfer function $T(k)$ and growth factor $D(z)$. The baryon content, and thereby BAO, is incorporated in $T(k)$ which can be approximately separated into the cold dark matter (CDM) and baryon components: $T(k) = (\Omega_b/\Omega_0)T_b(k) + (\Omega_c/\Omega_0)T_c(k)$, where Ω_c is the CDM density parameter relative to the critical density at present,

¹ National Astronomical Observatories, Chinese Academy of Sciences, Beijing 100012, China

² Graduate School of Chinese Academy of Sciences, Beijing 100049, China

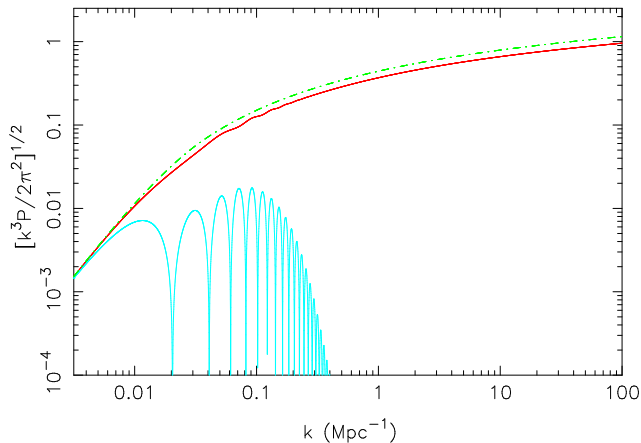


FIG. 1.— Linear matter power spectra at $z = 6$ for three different matter contents: pure CDM (dot-dashed line), pure baryons (grey) and mixed CDM+baryons (solid line). The BAO features can be seen at $k \sim 0.1 \text{ Mpc}^{-1}$ in the mixed matter model.

$\Omega_c = \Omega_0 - \Omega_b$. We adopt the asymptotic solutions to both $T_b(k)$ and $T_c(k)$ near the sound horizon given by Eisenstein & Hu (1998), in which the suppression effect of baryons on scales below the sound horizon is included. Nonetheless, the linear matter power spectrum becomes inaccurate at smaller scales and later cosmic time. We employ a halo model to evaluate the nonlinear power spectrum (see Cooray & Sheth 2002), which accounts for contributions from the single halo term P_{1h} plus the clustering term P_{2h} . We take the Press-Schechter formalism for the mass function of dark halos and the Navarro-Frenk-White (Navarro, Frenk & White 1996) profile for the matter distribution inside each halo. Employment of the nonlinear matter power spectrum instead of the linear one is crucial in the sense that BAO can be erased entirely on scales of nonlinear structures, although this may not be a serious problem at the epoch of reionization.

In Fig.1, we demonstrate the linear matter power spectra P_{lin} at redshift $z = 6$ for three matter contents: pure CDM, pure baryons and mixed CDM+baryons. Inclusion of baryons in the pure CDM model gives rise to the weak yet visible wiggles in the matter power spectrum at wavenumber $k \sim 0.1 \text{ Mpc}^{-1}$. Next, we calculate the nonlinear matter power spectrum instead of P_{lin} but leave the baryon content unchanged, and the result for $z = 6$ is shown in Fig.2. The nonlinear matter power spectrum at large scales $k < 1 \text{ Mpc}^{-1}$ remains roughly the same as P_{lin} , in which the weak BAO are clearly presented. The prominent nonlinear structures dominate the matter power spectrum only at short wavelengths of $k > 1 \text{ Mpc}^{-1}$. It turns out that by the end of cosmic reionization at $z \approx 6$, BAO are still unaffected by the formation of nonlinear structures. This arises because the gravitationally bound systems such as dark halos and their associated large-scale structures at $z = 6$ have sizes much smaller than the typical scales ($\sim 100 \text{ Mpc}$) of BAO. In other words, many of the interesting modes of BAO should leave their imprints on the matter power

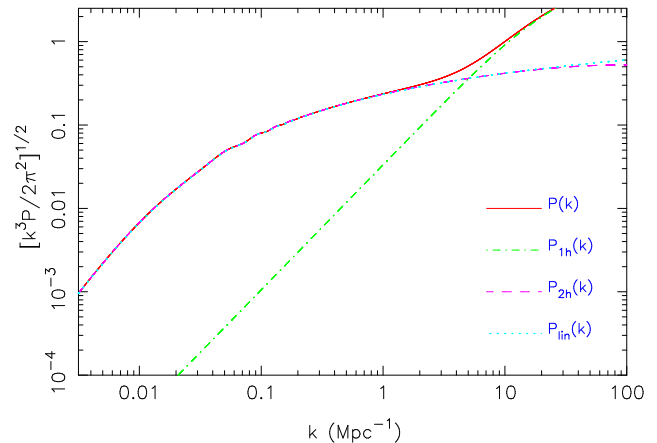


FIG. 2.— The matter power spectra at $z = 6$ predicted by linear density perturbation (dotted line) and halo model (solid line). For the latter, contributions of 1-halo and 2-halo terms are also displayed. Linear theory breaks down at small scales with wavenumber beyond $k > 1 \text{ Mpc}^{-1}$, and BAO are unaffected by nonlinear structures by $z = 6$.

spectrum before $z = 6$.

3. 21CM POWER SPECTRA

BAO signatures enter into the redshifted 21cm emission background from the epoch of reionization through the underlying matter density fluctuations (δ). If we restrict ourselves to the 21cm emission generated from the neutral hydrogen in the surroundings of the ionized bubbles of first-generation luminous objects, the surface brightness of the emission can be evaluated through (cf., Zaldarriaga, Furlanetto & Hernquist 2004)

$$\delta T_b \approx T_0(1 + \delta)(1 - x)$$

$$T_0 = 16 \text{ mK } h^{-1} \left(\frac{\Omega_b h^2}{0.02} \right) \left(\frac{1 + z}{10} \frac{0.3}{\Omega_M} \right)^{1/2}, \quad (1)$$

where $x = x_e(1 + \delta_x)$ is the ionization fraction, x_e is the average ionization fraction and δ_x is the perturbation in the ionization fraction across the sky, for which we will take the reionization model of Santos, Cooray & Knox (2005). The corresponding power spectrum of the 21cm emission can be written as

$$P_{21}^{3D}(z, k) = T_0^2 \left[(1 - x_e)^2 P_{\delta\delta}(z, k) + x_e^2 P_{\delta_x \delta_x}(z, k) - \left[2x_e(1 - x_e) P_{\delta\delta_x}(z, k) \right] \right]. \quad (2)$$

The three terms in the right-hand side represent the contributions of the matter power spectrum, the power from the perturbations in the ionization fraction, and the cross-correlation power, respectively. For the latter two, we use the model of Santos et al. (2003) to proceed our numerical computation. The angular power spectrum $C_\ell(\nu)$ of the redshifted 21cm brightness sky is derived under the flat-sky approximation.

The theoretically predicted 3D and 2D power spectra of the redshifted 21cm emission fluctuations are shown in Fig.3 and Fig.4, respectively. While the amplitudes

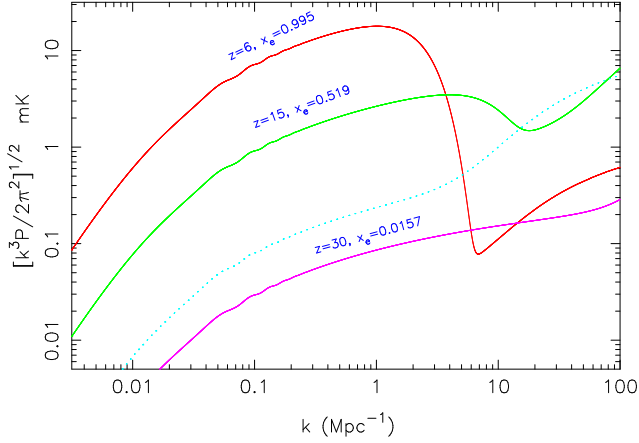


FIG. 3.— Power spectra of 21cm fluctuations at different redshifts from $z = 30$ to $z = 6$. The ionization fraction x_e is also showed at each redshift. BAO wiggles occur at $k \sim 0.1 \text{ Mpc}^{-1}$ and nonlinear structures dominate at $k > 1 \text{ Mpc}^{-1}$. The matter power spectrum at $z = 6$ is also plotted for comparison (dotted line).

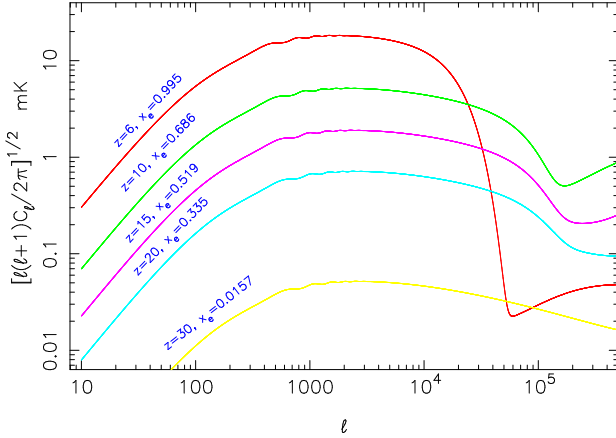


FIG. 4.— Angular power spectra of 21cm fluctuations at different redshifts from $z = 30$ to $z = 6$. BAO wiggles are presented at $\ell \approx 500 - 3000$, and their positions tend towards large ℓ with the increase of redshift.

of the 21cm power spectra themselves are relatively low, with a maximum value of $\sim 10 \text{ mK}$, the BAO induced wiggles are clearly presented. It appears that an angular resolution of $\sim 10 \text{ arcminute}$ is needed in order to identify the BAO features on the 2D power spectra, apart from the requirement of high sensitivity. Moreover, the positions of BAO tend towards large ℓ with the increase of redshift, indicating that radio arrays with baseline of $\sim 1 \text{ km}$ will be needed to reveal these structures. We have also calculated the 1D power spectrum of the 21cm emission along the line of sight but found that the BAO features are completely washed out due to projection effect, in agreement with the result of Wang & Hu (2006). Finally, it is pointed out that our analytical model does

not take the size distribution of ionized bubbles into account. The typical sizes of the ionized bubbles near $z \approx 6$ can reach $\sim 20 \text{ Mpc}$, which is already comparable to the BAO wiggles at large k or ℓ . Whether or not the ionized bubbles produce oscillations on the same scales as BAO should be investigated in future study.

4. DETECTABILITY

Detection of the BAO signatures on the redshifted 21cm fluctuations indeed poses a technique challenge for existing and planned low-frequency radio telescopes. We demonstrate the observability using 21 CentiMeter Array (21CMA, cosmo.bao.ac.cn), Low Frequency Radio Array (LOFAR, www.lofar.org) and Mileura Widefield Array (MWA, www.haystack.mit.edu/arrays/MWA), and only work with the angular power spectrum C_ℓ at a fixed frequency. Supposing that strong foreground contamination can be entirely removed from the low frequency sky through either the two-point correlation technique in frequency domain (e.g. Zaldarriaga, Furlanetto & Hernquist 2004) or the pixel-by-pixel algorithm (Wang et al. 2006), we can estimate the variance in C_ℓ through $\Delta C_\ell = [2/(2\ell + 1)f_{\text{sky}}]^{1/2}(C_\ell + N_\ell)$, in which $f_{\text{sky}} = \pi\theta_{\text{deg}}^2/129600$ accounts for the sky coverage, and $N_\ell = (wf_{\text{sky}})^{-1}e^{\theta_b^2\ell(\ell+1)}$ is the noise power spectrum if we adopt a Gaussian function with width θ_b for the experimental beam and use $w^{-1} = 4\pi\sigma_{\text{pix}}^2/N_{\text{pix}}$ to denote the contribution of the white noise with σ_{pix} and N_{pix} being the pixel noise and total number of pixels, respectively. In radio interferometric measurement, the pixel noise can be represented in terms of brightness temperature as $\sigma_{\text{pix}} = T_{\text{sys}}/\eta\sqrt{2N\Delta\nu t}$, where T_{sys} is the system temperature, η is the efficiency factor of telescope, N is the total number of independent baselines, $\Delta\nu$ is the bandwidth, and t is the observing time.

To proceed further, for 21CMA we take a system temperature of $T_{\text{sys}} = 250 \text{ K}$ and an efficiency of $\eta = 0.64$. The total dishes of 21CMA are $N_{\text{dish}} = 81$ and the longest baseline is 6 km , which gives rise to an angular resolution of $\theta_b \approx 1 \text{ arcmin}$. We use a conservative value of $\theta_b = 2 \text{ arcmin}$ in the present estimate. The sky coverage is, nevertheless, very small: $f_{\text{sky}} = 10^{-3}$. For LOFAR (compact core), the corresponding parameters are chosen to be: $T_{\text{sys}} = 100 \text{ K}$, $\eta = 0.64$, $N_{\text{dish}} = 32$, $\theta_b = 3 \text{ arcmin}$, and $f_{\text{sky}} \approx 0.1$. We utilize the following parameters for MWA: $T_{\text{sys}} = 200 \text{ K}$, $\eta = 0.64$, $N_{\text{dish}} = 500$, $\theta_b = 5 \text{ arcmin}$, and $f_{\text{sky}} \approx 0.4$. The errors ΔC_ℓ in the measurement of the 21cm power spectra with 21CMA, LOFAR (core) and MWA are displayed in Fig.5 for $z = 10$ and $z = 20$, respectively. While it is promising for all the three experiments to detect the reionization signals in the angular power spectra of 21cm fluctuations over a wide range of redshifts beyond $z = 6$ and angular scales from $\ell \sim 10^2$ to $\sim 10^4$, after an integration time of $\sim 1 \text{ year}$, a significant detection of the BAO wiggles on the 21cm angular power spectrum turns to be still difficult especially at higher redshifts (or lower frequencies) due to both the weak signals of BAO themselves and the limitation of angular resolutions of current radio telescopes. The strategy is that the maximum variations of BAO (e.g. the power difference between acoustic peaks and adjacent troughs) should exceed the

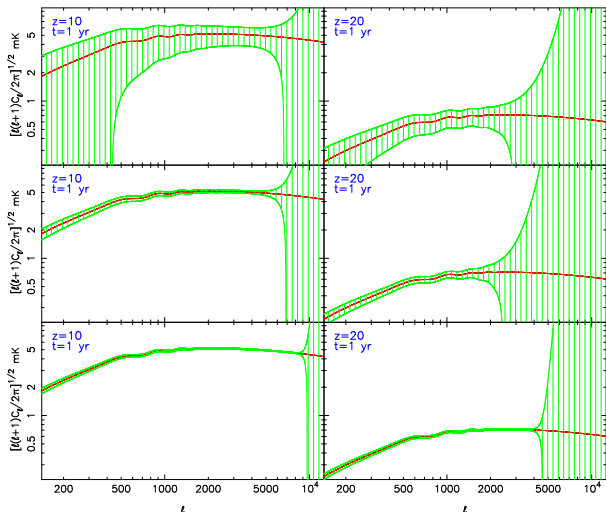


FIG. 5.— The expected angular power spectra and measurement errors with 21CMA (top), LOFAR(core) (middle) and MWA (bottom) for a bandwidth of $\Delta\nu = 0.1$ MHz and an integration time of 1 year.

errors at the corresponding modes. To optimize the detection, one should choose to work at higher frequencies near 200MHz, though the total 21cm signals may become weaker because the reionization process almost completed by $z = 6$. To be specific, the relatively smaller sky coverage and higher system temperature of 21CMA prevent a significant detection of the BAO wiggles on the angular power spectra of 21cm fluctuations unless a longer integration time of ~ 10 years is allowed. In contrast, both LOFAR and MWA may be able to capture the BAO signals within ~ 1 year. In particular, MWA can even trace all the BAO wiggles out to $z \approx 30$ and on very small angular scales of a few arcminutes because of its numerous independent baselines. We anticipate that a similar result can be reached when all the 77 stations in the planned LOFAR start to operate.

5. CONCLUSIONS

The BAO should be imprinted onto the 21cm emission background from the epoch of reionization through the underlying density perturbations. Detection of the signals will provide valuable information about the formation and evolution of cosmic structures at higher redshifts beyond $z \approx 6$. It also furnishes a standard ruler to the

probe of topology and geometry of the universe including dark energy and its equation of state. In particular, many of the BAO modes were not erased by the formation of large-scale structures by $z = 6$, and we may be able to see the BAO wiggles at smaller scales. This will complement our knowledge of the BAO at intermediate redshifts in addition to the detections of BAO signatures in CMB at $z \approx 1000$ and in large-scale distribution of galaxies at $z \approx 0$. A combination of these BAO measurements at different redshifts will allow us to set more robust constraints on the determinations of cosmological parameters.

We have used an analytic approach based on halo model for distribution and evolution of dark matter, in which baryons trace essentially dark matter but the standard CDM power spectrum is modified by the presence of baryons. We have then calculated the 21cm emission power spectrum from neutral hydrogen surrounding the ionized bubble of each halo, following a simple model of ionization history. Our results show that BAO are indeed presented at the power spectra of the redshifted 21cm emission from the epoch of reionization, and are almost unaffected by the presence of nonlinear structures beyond $z > 6$. This indicates that one should be able to see many of the BAO modes at the 21cm power spectrum.

We have worked with the angular power spectra of the 21cm emission from the epoch of reionization for a fixed frequency. The BAO signatures are clearly seen at $\ell \approx 500-3000$ through the entire history of reionization. However, detections of these wiggles with existing and planned radio interferometric arrays such as 21CMA, LOFAR and MWA does pose a technique challenge. The primary difficulty, apart from the extremely faint signals of 21cm emission themselves from the epoch of reionization and the strong foreground at low frequency, arises from the high system noise and the limitation of angular resolutions. Yet, within an integration time of about 1 year, it seems that both LOFAR and MWA are capable of capturing the BAO signatures at $\ell \sim 1000$, provided that the foreground contamination can be successfully removed.

We thank an anonymous referee for valuable comments and suggestions. This work was supported by the Chinese Academy of Sciences under grant KJCX2-YW-T02

REFERENCES

- Barkana, R., & Loeb, A. 2005, MNRAS, 363, L36
- Cole, S., Percival, W. J., Peacock, J. A., et al. 2005, MNRAS, 362, 505
- Cooray, A., & Sheth, R. 2002, Phys. Rep., 372, 1
- Eisenstein, D. J., & Hu, W. 1998, ApJ, 496, 605
- Eisenstein, D. J., Zehavi, I., Hogg, D. W., et al. 2005, ApJ, 633, 560
- Furlanetto, S. R., Sokasian, A., & Hernquist, L. 2004, MNRAS, 347, 187
- Hu, W., & White, M. 1996, ApJ, 471, 30
- Navarro, J. F., Frenk, C. S., & White, S. D.M. 1996, ApJ, 462, 563
- Santos, M. G., Cooray, A., Haiman, Z., Knox, L., & Ma, C.-P. 2003, ApJ, 598, 756
- Santos, M. G., Cooray, A., & Knox, L. 2005, ApJ, 625, 575
- Spergel, D. N., Bean, R., Doré, O., et al. 2007, ApJS, 170, 377
- Wang X., & Hu, W. 2006, ApJ, 643, 585
- Wang X., Tegmark, M., Santos, M. G., & Knox, L. 2006, ApJ, 650, 529
- Wyithe, S., Loeb, A., & Geil, P. 2007, arXiv:astro-ph/07092955
- Zaldarriaga, M., Furlanetto, S. R., & Hernquist, L. 2004, ApJ, 608, 622